Applied Energy 320 (2022) 119142

Contents lists available at ScienceDirect

Applied Energy

journal homepage: www.elsevier.com/locate/apenergy

A comprehensive and modular set of appliance operation MILP models for demand response optimization

Carlos Henggeler Antunes [a,b,*], Maria João Alves [a,c], Inês Soares [a]

[a] INESC Coimbra, DEEC, Rua Sílvio Lima, Pólo II, Coimbra 3030-290, Portugal
[b] Department of Electrical and Computer Engineering, University of Coimbra, Rua Sílvio Lima, Pólo II, Coimbra 3030-290, Portugal
[c] CeBER and Faculty of Economics, University of Coimbra, Av. Dias da Silva 165, Coimbra 3004-512, Portugal

HIGHLIGHTS

- Detailed energy consumption models for different appliance categories are developed.
- Modular models can be used as building blocks enhancing their flexibility.
- MILP models of appliance operation can be incorporated in energy management systems.
- Models allow for the integrated optimization of all energy resources.
- Models enable the participation in demand response programs.

ARTICLE INFO

Keywords:
Demand-side management
Load modeling
Demand response
Mixed-integer linear programming (MILP) models

ABSTRACT

Demand response programs are essential to enable accommodating larger shares of variable power generation based on renewable sources, the deployment of which is imperative for decarbonizing the economy and mitigating global warming. Consumers/prosumers are increasingly exposed to and may benefit from time-differentiated energy prices aimed to induce changes in regular consumption patterns. These changes are also beneficial for retailers and grid operators in face of the variability of wholesale market prices, renewable energy availability and grid conditions. The optimization models to be implemented in autonomous home energy management systems require a rigorous modeling of appliance operation to generate effective load scheduling solutions, respecting their physical operation principles and use patterns in everyday life. A balance should be sought between the detail level of optimization models and the computational requirements to generate usable solutions having in mind their implementation in low-cost processors. This paper presents a comprehensive and modular set of mixed-integer linear programming models aimed at enabling their seamless incorporation in home energy management systems, allowing for the integrated optimization of all energy resources (exchanges with the grid, load management, electric vehicle and stationary battery, local microgeneration). Detailed energy consumption optimization models for shiftable, interruptible and thermostatic loads are presented, also including the power cost component and ways of dealing with user's discomfort. The modular models are presented in a building block manner enhancing the flexibility of their utilization in overall models with different objective functions encompassing the economic and comfort dimensions. Computational results are presented for a case study using actual data, which considers a time-of-use tariff with six periods. In addition to comparing with a plain tariff scheme, different consumer profiles are simulated to assess the impact of comfort requirements on cost. These results show that whenever consumers have the flexibility to change their consumption patterns, they are able to lower the net electricity bill by having an energy management system endowed with the models herein proposed to make optimized decisions on their behalf.

* Corresponding author.
E-mail address: cantunes@inescc.pt (C. Henggeler Antunes).

https://doi.org/10.1016/j.apenergy.2022.119142
Received 21 December 2021; Received in revised form 25 February 2022; Accepted 14 April 2022
0306-2619/

1. Introduction

The increasing deployment of distributed generation based on renewable sources is essential to decarbonize the economy, mitigate global warming and, in countries without endogenous fossil resources, reduce the energy external dependence. Distinct, and sometimes conflicting, trends contribute to shaping the energy transition underway. The electrification of the transportation sector, including private and fleet vehicles, requires the ubiquitous deployment of battery chargers, including fast and superfast ones. Comfort requirements in buildings lead to increasing climatization loads. Consumers have a more active role in managing their energy resources, becoming *prosumers* who should globally optimize exchanges with the grid, load management, local microgeneration (namely rooftop photovoltaics, PV) and storage assets (static and electric vehicle batteries). The traditional grid, based on the *supply follows load* paradigm, is steadily evolving to smart grids facilitating a *load follows supply* operation, with the widespread deployment of sensing and control equipment particularly in the distribution grid, including smart meters at the customer premises offering bidirectional communication with the grid. This technological infrastructure and the amount of data it enables to gather allow for a more efficient grid management. In this setting, all tariff components (energy, power, network use) can become time-differentiated according to the variability of wholesale market prices, renewable energy availability and grid conditions (e.g., congestion in distribution transformers), thus inducing adequate changes in consumption patterns. Therefore, in face of these pervasive trends, demand response programs play a key role in the energy transition, offering potential benefits to multiple players.

Demand response programs may be broadly categorized as *price-based* and *incentive-based*. Price-based refers to time-differentiated rates that may display large variations leading consumers to modify load operation schedule to obtain bill savings without jeopardizing comfort. Incentive-based refers to schemes as direct load control, interruptible load contracts, peak time rebate, demand bidding/buy back emergency programs, capacity and ancillary service markets. Consumers can reduce the electricity bill adjusting consumption patterns by making the most of the integrated optimization of all energy resources according to their flexibility regarding the provision of the energy services required (laundry, hot water, electric mobility, etc.). Retailers can profit from offering a portfolio of time-differentiated tariffs to distinct consumer segments by making the most of the difference between wholesale and retail prices. Aggregators can develop new business models to provide demand response capability as a service to the grid. Grid operators can avoid power peaks, reducing losses and avoiding/postponing expensive network reinforcements. Generators can prevent operating expensive and less environmentally friendly peaking units.

The literature on simulation and optimization models devoted to the implementation of demand response is abundant. We mention some pertinent review papers offering extensive perspectives in the field with distinct emphases, as well as selected references of recent works proposing optimization models with different scopes and depth regarding appliance physical modelling. Siano [1] presents a survey of demand response potentials and benefits in smart grids, encompassing enabling technologies and systems, energy controllers and communication systems, including reference to industrial case studies and research projects. A broad review of demand response in smart grids is made in [2], which can be categorized according to control mechanisms (centralized vs. decentralized), stimuli (price vs. incentive based) and decisions (task scheduling vs. energy management). A review mainly from the standpoint of the optimization models and methods is offered in [3]. Beaudin and Zareipour [4] offer a literature review of modelling optimal scheduling of residential energy resources, considering device heterogeneity, occupants' objectives, consumption uncertainty and infrastructure implications, including methods as mathematical optimization, model predictive control, and heuristic control. The authors recognize the need to create a baseline for Home Energy Management Systems (HEMS) evaluation, allowing for modelling household devices and comfort, as well as providing data as consumption and occupancy patterns, and PV generation. Hussain and Gao [5] offer a review of demand response programs and propose a communication and computation-based demand response program for future grid systems, considering an inclined-block tariff and the consumers' income and consumption profiles. Morales-España et al. [6] address demand response mainly from the power system perspective, including definitions and classifications of different types of demand response, the products and services it can provide for energy, capacity and ancillary services. The authors also present simple optimization models for aggregated flexible load management involving curtailment and/or shifting.

Several authors proposed specific optimization models for demand response. Althaher et al. [7] consider that it is critical including in the models consumer satisfaction (e.g., volume of curtailed energy) in addition to minimizing electricity payments; however, the relation between the volume of curtailed energy and consumer's (dis)satisfaction is arguable since it should refer to the quality of the energy service being provided by loads (as proxied by hot water temperature, indoor comfort temperature, time of operation, etc.) and not to the volume of energy itself. The importance of reducing the computational complexity of the decision models embedded in energy management systems has been recognized in [8]. The aim is enabling the models to be solved on low-cost hardware to massify the implementation of HEMS. In [9], it is considered that a price-based model requires lower computational capabilities than an incentive-based model at the expense of less certainty of the response from the loads to the price signals. Nan et al. [10] propose a scheduling scheme for the dispatch of residential loads by an aggregator, considering the minimization of the electricity consumption cost, the peak load, the peak-valley difference and the users' discomfort, through which residential communities can participate in demand response programs. Adhikari et al. [11] present a direct load control approach for a set of heating, ventilation and air conditioning (HVAC) units to maximize the load reduction potential during a demand response period, considering indoor temperatures within individual consumers' preference bounds and transforming the control problem into a job scheduling problem. Shafie-Khah and Siano [12] present a stochastic model of a HEMS guaranteeing the users' satisfaction by means of a response fatigue index, also accounting for uncertainties of electric vehicles availability for charging/discharging and local renewable energy generation. Elkazaz et al. [13] present a hierarchical two-layer HEMS to minimize daily household energy costs by means of a model predictive controller using a mixed-integer linear programming (MILP) model to determine the operating schedule for shiftable domestic appliances and the profile for energy storage for the next 24 h, and maximize photovoltaic self-consumption using a rule-based real-time controller to determine the optimal settings of the battery storage system compensating for the effects of forecast uncertainties and sample time resolution. Javadi et al. [14] develop a self-scheduling model for a HEMS including a linear discomfort index encompassing the end-users' preferences in the daily operation of home appliances. The problem is modelled as a multi-objective MILP model, considering the minimization of the energy bill and the discomfort index to determine the optimal time slots for appliance operation. Zhang et al. [15] propose a conceptual architecture of a price-based demand response management controller implementing a multi-agent reinforcement learning-based algorithm to optimize the energy consumption of various devices. Mohseni et al. [16] develop an energy consumption model of home appliances based on the "set of sequential uninterruptible energy phases" approach, in a residential microgrid equipped with PV generation, battery storage systems and electric vehicles, to activate time-based demand response programs in day-ahead planning.

Two fundamental dimensions are at stake for evaluating the merit of solutions to this type of models: minimizing cost and discomfort. The cost refers to energy and power costs and may also include a revenue component if selling back to the grid is allowed using some remuneration scheme. Energy costs (€/kWh) result from a time-of-use (ToU) tariff scheme contracted between the retailer and the consumer for a specified period (e.g., one year), which can be dynamic in the sense of being announced at short notice (for instance, 24 or 48-hour ahead). Power costs (€/kW per day) result from a contracted limit power or a scheme in which the consumer pays for the maximum power taken during a certain period (e.g., one hour or one day). The discomfort can be assessed by means of several axes associated with the quality of the energy service to be provided: time, regarding the most preferred periods for the operation of some appliances (e.g., washing machine); temperature, concerning the comfort ranges for indoor or water temperatures; state of charge of electric vehicle (or static) battery.

The cost and discomfort dimensions can be incorporated in the models by means of objective functions to be minimized, as constraints or in a mixed way. The model can consider an objective function minimizing costs of energy and power subject to constraints expressing the comfort thresholds acceptable by the consumer, which would indicate a more economic-oriented consumer. The model can, instead, consider an objective function minimizing discomfort, in general representing deviations from a user-specified comfort setting or range, e.g., number of minutes of load operation postponement beyond the desired time, indoor/water temperature outside a desired range, or state of charge of the electric vehicle battery below the required value. The discomfort can also be monetized, i.e., the cost assigned by the consumer to a certain postponement in operation or temperature degree above/below the preferred setting, subject to a budget constraint. The monetization of discomfort allows for considering an overall cost objective function involving different components. Moreover, multiobjective models explicitly considering cost and discomfort objective functions can be developed, which enable deriving a Pareto optimal frontier of solutions displaying different tradeoffs between the competing objectives [17].

Some approaches consider a utility function to be maximized, which is a proxy for the level of satisfaction with the energy services delivered, in general directly associated with (the perceived benefit of) energy consumption, or a disutility cost associated with the load suppressed [18]. Quadratic utility functions are often used to model individual consumer's preferences, displaying linear decreasing marginal benefit related to energy consumption [19,20]. However, the elicitation of realistic utility functions characterizing the consumer's satisfaction, as a result of the energy consumed by each appliance providing an energy service, is problematic in practice and does not capture explicitly the decisions at appliance level. The use of functions penalizing the deviation to an expected "optimal" consumption value is also not representative of users' energy behaviors. Hence, demand response optimization models ought to incorporate the physical characteristics and type of control of each load, as well as typical operation patterns, time slots and comfort settings preferred for operation. A compromise should be established between the accurate load operation and control modeling and the computational effort to solve the models, particularly with fine-grain time discretization, due to the models' combinatorial nature.

The integrated optimization of all energy resources (exchanges with the grid, loads, storage, microgeneration) requires the design of Autonomous Home Energy Management Systems (AHEMS) located behind the meter, which are endowed with optimization models and algorithms capable of making 24/7 decisions on the consumer's behalf. For this purpose, it is necessary to develop thorough load operation mathematical programming models to be tackled by optimization algorithms so that effective operational solutions are obtained. These models should respect the physical operation and control principles of the appliances as well as their habitual utilization patterns in everyday life. The accurate physical-based load operation modelling may require many binary variables and constraints, which makes more difficult to obtain an optimal solution (single objective models) or Pareto optimal solutions (multiple objective models) in an acceptable computation time. Therefore, a balance should be sought between the modeling detail level and the computational requirements to obtain practical solutions, having in mind their implementation in AHEMS running on low-cost processors. According to the type of control, residential loads can be categorized in *shiftable* (the operation cycle cannot be interrupted), *interruptible* (can be interrupted and resume operation at a later stage), and *thermostatic* (controlled by a state variable such as indoor temperature) loads [21].

Although the literature in optimization models for demand response is vast, many models presented in the literature consider a number of simplifications that deviate them from the reality. Thus, there is a lack of effective physical-based models. The models we present in this paper are the result of an in-depth study of the appliance operation, taking into account several parameters such as: operation cycles requiring different power at different stages, the behavior of a thermostat with hysteresis, main principles of heat transfer in buildings, etc. The main contributions of this paper are the following:

- development of a comprehensive and modular set of MILP models of appliance operation that are aimed at being seamlessly incorporated in AHEMS allowing for the integrated optimization of all energy resources;
- development of detailed energy consumption models for each load category;
- consideration of different cost objective function components (energy and power costs, and monetized discomfort) as well as ways of dealing with the possible user's discomfort derived from operating appliances out of the habitual periods/settings and/or temperature ranges;
- assessment of the computational efficiency in real settings considering a fine-grain time discretization (1 min);
- for shiftable loads, alternative models have been developed and compared to determine the most efficient one;
- the modular models are developed in a building block manner enhancing the flexibility of their utilization in overall models with different objectives encompassing the economic and comfort dimensions.

To the best of our knowledge, such a consistent and complete set of models is for the first time presented in the literature, which includes the accurate modeling of a large diversity of energy resources and exchanges with the grid (buying and selling electricity) that can be used according to different needs.

This work contributes for the development of reliable AHEMS that can be parameterized with the user's preferences to optimally manage all energy resources on behalf of consumers engaged in profiting from the benefits of demand response programs. Moreover, the detailed optimization models are key to retailers interested in offering time-of-use tariff schemes to anticipate the consumers' reaction, which is an essential step for tariff design (prices and time periods in which they apply) [22].

Section 2 presents the materials and methods, establishing a common framework for the modular models presented in the subsequent sections. Section 3 is devoted to specific models for: 1) shiftable loads, 2) electric water heater model including sanitary constraints, 3) air conditioner based on the indoor temperature dynamics, 4) static and electric vehicle batteries. An overall optimization model is presented in Section 4 encompassing exchanges (buying, selling) with the grid, shiftable loads, electric water heater, air conditioner, static and electric vehicle batteries, as well as microgeneration. The overall model was applied to a case study, including a comparison of a ToU tariff and a plain tariff equal to the average price of the ToU tariff. A sensitivity analysis is also carried out to assess the impacts on cost of consumers being more or less willing to tolerate some discomfort, e.g., changing the minimum allowable indoor temperature or the reference hot water temperature. The main conclusions are drawn in Section 5.

2. Materials and methods

Specific accurate models are developed for shiftable loads, electric water heater (EWH), air conditioner system (AC), static battery and electric vehicle (EV) battery.

The planning period (e.g., one day) is discretized in time intervals with equal length.

Shiftable loads are characterized by an operation cycle associated with each program (energy service), which cannot be interrupted. Examples are laundry machines, dishwashers and cloth dryers. Models considering that an appliance is supplied with a given amount of energy for service completion (as if the power required was constant, instead of a load diagram with diversified stages) are rather simplistic and ultimately useless for optimization purposes. The consideration of the operation cycle (e.g., in a laundry machine, consisting of heating water, spinning and drying phases) is essential because this is the actual physical functioning and the power required at each phase is significantly different. Therefore, for each shiftable load, in the models proposed herein,

- the technical inputs are the operation cycle duration and the power required at each operation stage;
- the consumer should provide the comfort time slots for load operation according to his/her preferences, which may be disjoint in the planning period;
- the optimization determines the starting operation time and guarantees that the cycle is entirely executed in the due sequence within any of the comfort time slots, correctly mapping the operation cycle onto the planning period.

In our previous works, the model we developed to accurately representing the functioning of shiftable appliances requires a high number of binary variables and constraints (the model was first proposed in [23] and also used in other works, e.g. in [24]). We propose herein two alternative more efficient models, which will be compared with the former one.

The EWH is an important load in most homes, accounting for a significant share of energy consumption. The appliance rated power may vary in a large range from 1500 W to 6000 W depending on the volume, which should be adapted to the number and habits of inhabitants. The EWH operation is controlled by a thermostat. In our previous works, the EWH has been dealt with in a more straightforward manner as an interruptible appliance, i.e., a certain amount of energy (a surrogate for the quality of service provided by hot water) should be supplied in a certain comfort time slot, so that the control was modeled using binary variables stating the *on/off* supply status [24]. The present model considers the water withdrawal and supply as well as sanitary constraints to avoid the formation of legionella bacteria, which requires heating the water to a safety temperature for a specified time. Therefore, in the EWH model proposed herein,

- the technical inputs are the power of the heating element, the ambient and inlet water temperatures, the tank characteristics (capacity, thermal characteristics of the envelope), and the period during which the water should be heated up to a certain temperature to eliminate the bacteria;
- the inputs provided by the consumer include the minimum and maximum allowed temperatures, and the water withdrawals (time and quantity);
- the optimization determines the on/off status of the heating element, which defines the hot water temperature in the tank.

HVAC systems contribute significantly to residential electrical energy consumption. The thermal inertia of indoor spaces makes these systems an appropriate target for control by making the most of time-differentiated tariffs and the flexibility of consumers to accept some deviation of the indoor temperature to the desired one for a limited period of time. The model developed in [25] is considered herein, which accounts for the behavior of the control thermostat with hysteresis of an AC system. In this model,

- the technical inputs are the nominal power and the coefficient of performance of the AC, the outdoor temperature and the thermal characteristics of the building envelope;
- the inputs provided by the consumer are the minimum and the maximum comfort indoor temperatures;
- the optimization determines the on/off status of the AC, which defines the indoor temperature.

The optimization of the operation of the static battery and the electric vehicle (EV) battery deals with the energy exchanges, to be integrated in the overall optimization of all energy resources. The static battery is, in principle, always available, whereas the EV battery is only available when the EV is at home and imposes further constraints in its utilization in vehicle to grid (V2G) mode considering the expected energy service (mobility) to be provided according to the consumer's needs. In the model proposed herein,

- the technical inputs are the charging and discharging efficiencies, the minimum and maximum allowed battery charges, and the minimum and maximum charge and discharge powers;
- the input set by the consumer is the battery charge requested at the departure time of the EV;
- the optimization determines the charging and discharging patterns of the static and EV batteries.

A base load not deemed for control and local PV generation are also considered in the overall model.

From the optimization process of the overall model, it results the power required for the operation of the shiftable loads, the EWH and the AC, in each time interval, as well as the battery charge and discharge, and the exchanges between the grid and the home.

We consider a planning period (e.g., one day) consisting of T time intervals each with a length Δt, indexed by $t = 1, \cdots, T$. We denote as time t the interval from $t-1$ to t. The length Δt depends on the time discretization adopted (typical values are $\Delta t = 1,\ 5$ or 15 min). In order to capture the actual operation of some appliances, namely the shiftable loads that have operation phases of short duration with a significant power required, a fine grain discretization (e.g., 1 min or 5 min) is advisable. In the analysis of the case study presented below, the planning period is discretized in intervals of 1 min, so $\Delta t = 1/60$h; therefore, $T = 1440$ for a planning period of 24 h. A ToU tariff is used with 6 different pricing periods. These prices are input data, which are denoted in the models by C_t^{buy}. The objective function of the overall model applied to the case study in Section 4 consists of minimizing the net cost, also considering the power cost component associated with the peak power required from the grid.

Models are of the MILP type due to the need of incorporating discrete variables to model *on/off* states, discrete operation power levels, and enforcing logical conditions to guarantee model consistency. Therefore, these models can be solved using a state-of-the-art MILP solver. In this work, the models were solved using the CPLEX solver. In this type of strongly combinatorial models with a large number of interdependent constraints but in which all the functions are linear, using a general MILP solver is advantageous over meta-heuristics because it can guarantee an optimal or near-optimal feasible solution. Experiments we have carried out using meta-heuristics customized for the modular models did not provide good results in terms of computational efficiency and solution quality.

All the data necessary to reproduce the results of the case study presented in Section 4 are available at https://home.deec.uc.

pt/~ch/data_DRmodels.

All the results were obtained in a computer with an Intel Xeon Gold 6138 CPU@3.7 GHz processor.

3. Models for demand response optimization

This section aims to present MILP models devoted to the different types of loads considering their physical operation principles and control modes: 1) shiftable loads, 2) electric water heater model including sanitary constraints, 3) air conditioner based on the indoor temperature dynamics, and 4) static and electric vehicle batteries.

3.1. Models for shiftable load operation

Let us consider J shiftable loads indexed by $j \in \{1, \cdots, J\}$, each one having a specific load diagram, as illustrated in Fig. 1, for which the input data are:

d_j = duration of load j operation cycle;

g_{jr} = power requested by load j at stage (time) r of its operation cycle ($r = 1, \cdots, d_j$).

The actual operation cycle is, therefore, discretized according to the Δt considered.

Let $[T_{L_j}, \cdots, T_{U_j}]$ be the time slot allowed by the consumer for the operation of load j.

In the first MILP model we proposed for shiftable appliances ([24,23]), the control is defined by binary variables with three indexes: $w_{jrt} = 1$ if load j is *on* at stage r of its operation cycle in time t of the planning period (within the allowed time slot), and $w_{jrt} = 0$ otherwise, i.e., it is *off*.

The auxiliary variables P^{Sh}_{jt} (where the superscript *Sh* denotes “shiftable”) denote the power requested to the grid by shiftable load j in time t of the planning period (kW), $j = 1, \cdots, J$, $t = 1, \cdots, T$. The power P^{Sh}_{jt} is zero for t outside the allowed time slot $[T_{L_j}, \cdots, T_{U_j}]$.

The constraints modeling the load operation guarantee that: each load j operates exactly once at stage r and this should occur within its comfort time slot (1); at each time t of the planning period, each load j may be *off* or *on* only at one stage r of its operation cycle (2); if load j is *on* in time t and at stage $r < d_j$ of its operation cycle, then it must also be *on* in time $t+1$ and stage $r+1$, for $r = 1, \cdots, d_j - 1$ (3); load j should start its working cycle at most in time $T_{U_j} - d_j + 1$, thus assuring that it never finishes later than T_{U_j} (4). These constraints also ensure that load j will operate only once. Constraints (5) and (6) set the value of the power requested to the grid by each load j in each time t. This model (presented in [23]) is denoted as M1 below.

$$\sum_{t=T_{L_j}}^{T_{U_j}} w_{jrt} = 1 \ , \ j = 1, \cdots, J \ , \ r = 1, \cdots, d_j \tag{1}$$

$$\sum_{r=1}^{d_j} w_{jrt} \leq 1 \ , \ j = 1, \cdots, J \ , \ t = T_{L_j}, \cdots, T_{U_j} \tag{2}$$

$$w_{j(r+1)(t+1)} \geq w_{jrt} \ , \ j = 1, \cdots, J \ , \ r = 1, \cdots, (d_j - 1) \ , \ t = T_{L_j}, \cdots, (T_{U_j} - 1) \tag{3}$$

$$\sum_{t=T_{L_j}}^{T_{U_j}-d_j+1} w_{j1t} = 1 \ , \ j = 1, \cdots, J \tag{4}$$

$$P^{Sh}_{jt} = \sum_{r=1}^{d_j} g_{jr} w_{jrt} \ , \ j = 1, \cdots, J \ , \ t = T_{L_j}, \cdots, T_{U_j} \tag{5}$$

$$P^{Sh}_{jt} = 0 \quad , \ j = 1, \cdots, J \ , \ t < T_{L_j} \vee t > T_{U_j} \tag{6}$$

$$w_{jrt} \in \{0, 1\} \ , \quad j = 1, \cdots, J \ , \quad r = 1, \cdots, d_j \ , \quad t = T_{L_j}, \cdots, T_{U_j} \tag{7}$$

Since model M1 requires a large number of binary variables for each load j, as many as $(T_{U_j} - T_{L_j} + 1) \times d_j$, we propose herein and compare the performance of two other approaches for modeling the operation cycle of shiftable load. The idea is to define binary variables just to determine the starting time of each load j:

$$s_{jt} = \begin{cases} 1 & \text{if load } j \text{ begins its operation in time } t \\ 0 & \text{otherwise} \end{cases} \quad j = 1, \cdots, J; t = T_{L_j}, \cdots, T_{U_j} - d_j + 1$$

In a first approach using variables s_{jt} – denoted below as model M2 – the operation cycle is enforced by data organization in a matrix $D^j_{tt'}$: each element of $D^j_{tt'}$ indicates the power (kW) requested by load j in time t' if the load starts operating in time t, for all pairs (t, t') with $t = T_{L_j}, \cdots, T_{U_j} - d_j + 1$, $t' = T_{L_j}, \cdots, T_{U_j}$. Then, the power required is computed as in (8). Thus, model M2 is defined by constraints (8)–(11).

$$P^{Sh}_{jt'} = \sum_{t=T_{L_j}}^{T_{U_j}-d_j+1} D^j_{tt'} . s_{jt} \quad , \quad j = 1, \cdots, J, \quad t' = T_{L_j}, \cdots, T_{U_j} \tag{8}$$

$$\sum_{t=T_{L_j}}^{T_{U_j}-d_j+1} s_{jt} = 1 \quad , \quad j = 1, \cdots J \tag{9}$$

$$P^{Sh}_{jt} = 0 \quad , \ j = 1, \cdots, J \ , \ t < T_{L_j} \vee t > T_{U_j} \tag{10}$$

$$s_{jt} \in \{0, 1\} \ , \quad j = 1, \cdots, J, \quad t = T_{L_j}, \cdots, T_{U_j} - d_j + 1 \tag{11}$$

For the sake of illustration, let us suppose that load j has the allowed time slot $[T_{L_j}, T_{U_j}] = [10, 17]$ with $d_j = 3$ (i.e., 45 min considering Δt = 15 min), and g_{jr} $(r = 1, \cdots, 3)$ given by $g_{j1} = 1.2$, $g_{j2} = 1.5$, $g_{j3} = 0.5$, in kW.

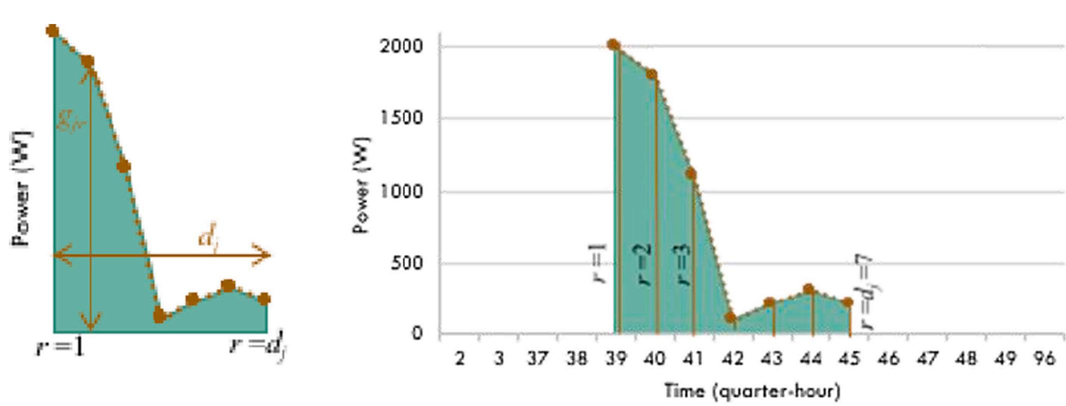

Fig. 1. Operation cycle of shiftable load j consisting of d_j stages with power g_{jr} required at each stage r.

Matrix $D^j_{tt'}$ is defined for t in $T_{L_j} = 10, \ldots, T_{U_j} - d_j + 1 = 15$ and $t' = 10, \ldots, 17$, as:

(t,t′)	t′ = 10	11	12	13	14	15	16	17
t = 10	1.2	1.5	0.5	0	0	0	0	0
11	0	1.2	1.5	0.5	0	0	0	0
12	0	0	1.2	1.5	0.5	0	0	0
13	0	0	0	1.2	1.5	0.5	0	0
14	0	0	0	0	1.2	1.5	0.5	0
15	0	0	0	0	0	1.2	1.5	0.5

This matrix can be built with the optimization solver programming language (e.g., in CPLEX or Gurobi) or read once just at the beginning of the run from a pre-prepared data file.

It is straightforward to expand this data matrix accommodating multiple operation slots, i.e. considering that load j can operate in not just one but multiple slots, defined by the consumer according to his/her convenience:

$\mathrm{T}(j) = \left[T^1_{L_j}, T^1_{U_j}\right] \cup \left[T^2_{L_j}, T^2_{U_j}\right] \cup \cdots \left[T^{a_j}_{L_j}, T^{a_j}_{U_j}\right] \subseteqq \mathrm{T}$ defines the time slots in which each load $j \in \{1, \cdots, J\}$ can operate, where a_j is the number of different disjoint periods allowed for the operation of load j. It is assumed that load j will operate only once, so it will operate within only one of these time slots in $\mathrm{T} = \{1, \cdots, T\}$.

In this case, $D^j_{tt'}$ is defined for the combinations (t,t') considering the lowest time ($T^1_{L_j}$) for the beginning of rows and columns, the highest time of the union of the different slots for t' ($T^{a_j}_{U_j}$) and the highest possible starting time for t ($T^{a_j}_{U_j} - d_j + 1$). For instance, if load j has a cycle with $d_j = 2$ and can operate in slots [3–7] or [9–12] in a planning period $t = 1, \cdots, 20$, then matrix $D^j_{tt'}$ is defined for $t = 3, \ldots, 12\text{–}2 + 1 = 11$ and $t'=3, \ldots, 12$. The elements $D^j_{tt'} = 0$ for t and t' in between the two allowed time slots.

Model M2 has the advantage over M1 of requiring fewer binary variables. However, it is necessary to organize *a priori* the D^j matrices from the $g_{jr}, r = 1, \cdots, d_j$, and the time slots data. Therefore, another model is proposed, which considers the same type of variables s_{jt} as in model M2 but does not require the D^j matrices. This model is denoted as M3.

Let us firstly consider only one operation time slot $\left[T_{L_j}, T_{U_j}\right]$ for each load j. The constraints impose that: load operation should start once, enabling the cycle to end within the allowed time slot - (9) and (11); map the power required by shiftable load j at each stage of the operation cycle onto the planning period (i.e., $g_{jr} \rightarrow P^{Sh}_{jt}$), according to the starting time by defining the new constraints (12), which have the role of (8) in M2; $P^{Sh}_{jt} = 0$ for t outside the allowed time slot - (10).

Let $R(j) = \{1, \cdots, d_j\}$.

$$P^{Sh}_{jt} = \sum_{r \in R(j): r \le t \wedge r \le t+1-T_{L_j}} g_{jr} \cdot s_{j(t-r+1)}, \qquad j = 1, \cdots, J, \quad t = T_{L_j}, \cdots, T_{U_j} \tag{12}$$

Constraints (12) define the power P^{Sh}_{jt} required by load j in each time t of its allowed operation slot. Let us explain how these constraints ensure this purpose: suppose that load j starts to operate at $t' \in \left[T_{L_j}, T_{U_j} - d_j + 1\right]$, i.e., $s_{jt'} = 1$ and $s_{jt} = 0, \forall t \ne t'$; at $t = t'$, load j should operate at $P_{jt'} = g_{j1}$, because it is at stage $r = 1$ of its operation cycle; at $t = t' + 1$, load j should operate at $P_{j,t'+1} = g_{j2}$, because $r = 2$, and so forth; for $t = t'$, the only r in which $s_{j(t'-r+1)} = 1$ is for $t' - r + 1 = t'$, i.e. $r = 1$; for $t = t' + 1$, the only r in which $s_{j(t'+1-r+1)} = 1$ is for $t' + 1 - r + 1 = t'$, i.e. $r = 2$; and so forth. In the summation in (12), r must satisfy $r \le t \wedge r \le t+1 - T_{L_j}$ to ensure that only existing variables are considered in $s_{j(t-r+1)}$. Note that for $r = t+1$ those variables become s_{j0}, and for $r = t - T_{L_j} + 2$ the variables would be $s_{j(T_{L_j}-1)}$ which do not exist.

Model M3 can also be extended considering that load j can operate in multiple slots $\mathrm{T}(j) = \left[T^1_{L_j}, T^1_{U_j}\right] \cup \left[T^2_{L_j}, T^2_{U_j}\right] \cup \cdots \left[T^{a_j}_{L_j}, T^{a_j}_{U_j}\right]$. The constraints should now account for the multiple slots a_j.

Let $\mathrm{T}start(j) = \left[T^1_{L_j}, T^1_{U_j} - d_j + 1\right] \cup \left[T^2_{L_j}, T^2_{U_j} - d_j + 1\right] \cup \cdots \cup \left[T^{a_j}_{L_j}, T^{a_j}_{U_j} - d_j + 1\right]$, which defines the times in which load j can start to operate.

The decision variables s_{jt} are defined as above but $t \in \mathrm{T}start(j)$. The constraints of M3 for multiple slots are (13)–(16).

$$\sum_{t \in \mathrm{T}start(j)} s_{jt} = 1, \qquad j = 1 \cdots J \tag{13}$$

$$P^{Sh}_{jt} = \sum_{\substack{r \in R(j): r \le t \ \wedge \\ r \le t+1-T^a_{L_j},\ a=1,\cdots,a_j}} g_{jr} \cdot s_{j(t-r+1)}, \qquad j = 1, \cdots, J, \quad t \in \mathrm{T}(j) \tag{14}$$

$$P^{Sh}_{jt} = 0, \qquad j = 1, \cdots, J, \quad t \notin \mathrm{T}(j) \tag{15}$$

$$s_{jt} \in \{0, 1\}, \qquad j = 1, \cdots, J, \quad t \in \mathrm{T}start(j) \tag{16}$$

In addition to the typical shiftable loads generally considered (laundry, drying, dishwasher), other shiftable loads can be considered, including the ones that do not have an operation cycle, have constant operation power and can be interrupted, but the consumer wants them to operate in continuous periods (e.g., ironing).

These three models (M1-M3) of shiftable loads have been compared considering as objective function the minimization of the energy consumption cost:

$$\min\ cost = \sum_{t=1}^{T} \sum_{j=1}^{J} C^{buy}_t\ P^{Sh}_{jt}\ \Delta t \tag{17}$$

where C^{buy}_t are the energy prices (cents €/kWh), $t = 1, \cdots, T$.

Three types of shiftable loads are considered: dishwasher ($j = 1$, $\left[T_{L_1}, T_{U_1}\right]$=[1,480], d_1=90), laundry ($j = 2$, $\left[T_{L_2}, T_{U_2}\right]$=[406,870], d_2=105), dryer ($j = 3$, $\left[T_{L_3}, T_{U_3}\right]$=[1126,1440], d_3=220). The data used for the three loads in this experiment are the same as the data for the shiftable loads in the case study (Section 4).

The comparison of the 3 models described above, considering just one comfort slot, is displayed in Table 1, revealing the clear advantage of M3. All models have 4320 continuous variables. The optimal cost of 0.47013 € was obtained in all models, but with a significant difference in runtime, which is quite relevant for real-time optimization.

3.2. Model for electric water heater

The *on/off* status of the resistive element of an EWH, typically with a constant power, should consider the simulation of water withdrawal according to a given consumption pattern, inlet water temperature and losses through the envelope. In addition to thermal exchanges, the optimization model considers sanitary constraints to avoid the formation of legionella bacteria, which requires heating the water to a safety temperature for a specified time. This is modeled imposing that the water temperature is above 60 °C for at least 11 consecutive minutes or above 75 °C for at least 3 consecutive minutes in each day [26].

The modeling of an EWH requires the following parameters and data:

P^R = power of the resistive heating element (kW).

τ^{amb}_t = ambient temperature around the EWH in time t (°C), $t = 1, \cdots,$

Table 1
Comparison of the shiftable load optimization models.

	M1	M2	M3
# Binary var	110,925	1008	1008
Runtime (s)	91.238	1.952	0.162

T.

τ^{net} = inlet water temperature (°C).

m_t = water withdrawal for consumption in time t (kg), $t = 0, \cdots, T$.

M = hot water tank capacity (kg).

A = area of the tank envelope (m^2).

U = heat transfer coefficient of the tank (W/m^2.°C).

c^p = specific heat of the water (J/kg.°C).

τ^{min}, τ^{max} = *minimum* and *maximum* allowed temperature (°C).

t^{req} = time required to maintain a certain temperature to eliminate the bacteria (min.).

τ^{req} = temperature specified to be kept for t^{req} to eliminate the bacteria (°C).

Decision and auxiliary variables (all for $t = 1, \cdots, T$):

v_t = binary variable defining the *on/off* control of the heating element in time t (v_0 is a constant).

τ_t = hot water temperature inside the tank in time t (°C), (τ_0 is a constant).

n_t = binary variable equal to 1 in the first t in which $\tau_t > \tau_{req}$ for t_{req}.

P_t^{losses} = power losses through the envelope in time t (kW), (P_0^{losses} is a constant).

The EWH optimization model is:

$$\min \sum_{t=1}^{T} \left(C_t^{buy} P^R v_t \Delta t \right) \tag{18}$$

s.t.

$$P_t^{losses} = A.U\left(\tau_t - \tau_t^{amb}\right), t = 1, \cdots, T \tag{19}$$

$$\tau_{t+1} = \left(\frac{M - m_t}{M}.\tau_t + \frac{m_t}{M}.\tau^{net} \right) + \frac{P^R v_t - P_t^{losses}}{Mc^p}.\Delta t, \quad t = 0, \cdots, T-1 \tag{20}$$

$$\tau_t \geq \tau^{min} - \mathscr{M} v_t, t = 1, \cdots, T \tag{21}$$

$$\tau_t \leq \tau^{max} + \mathscr{M}(1 - v_t), t = 1, \cdots, T \tag{22}$$

$$\sum_{t=1}^{T - t^{req} + 1} n_t = 1 \tag{23}$$

$$\tau_t \geq \sum_{\substack{t' = 1 \\ (t' \leq t)}}^{t^{req}} \tau^{req}.n_{t-t'+1}, t = 1, \cdots, T \tag{24}$$

$$v_t \in \{0, 1\}, n_t \in \{0, 1\}, t = 1, \cdots, T \tag{25}$$

$$P_t^{losses} \geq 0, \tau_t \geq 0, t = 1, \cdots, T \tag{26}$$

Constraints (19) and (20) define the temperature inside the tank. Constraints (21) and (22) enable that the minimum temperature may not be respected when the water is being heated ($v_t = 1$), to account for cases in which the initial temperature $\tau_0 < \tau_t^{min}$ or there is excessive withdrawal, as well as allowing for $\tau_t > \tau^{max}$ when $v_t = 0$. $\mathscr{M}$ is a big positive number. These constraints become hard, i.e., $\tau_t \geq \tau^{min}$ and $\tau_t \leq \tau^{max}$, if the EWH is *off* or *on*, respectively. Constraints (23) and (24) ensure that the temperature is τ^{req} or above for at least t^{req} consecutive times to avoid the legionella bacteria.

If the consumer is willing to withstand some discomfort with respect to a range of hot water temperatures $[\tau^{min-comf}, \tau^{max-comf}]$, penalizing the corresponding deviation in the objective function, then the following constraints could be considered:

$$\tau_t^{dev} \geq \tau^{min-comf} - \frac{(\tau_t + \tau_{t-1})}{2}, \quad t = 1, \cdots, T \tag{27}$$

$$\tau_t^{dev} \geq \frac{(\tau_t + \tau_{t-1})}{2} - \tau^{max-comf}, \quad t = 1, \cdots, T \tag{28}$$

$$\tau_t^{dev} \geq 0, \quad t = 1, \cdots, T \tag{29}$$

The temperature deviation variables τ_t^{dev} measure, in each time t, the degrees °C of the water temperature below $\tau^{min-comf}$ or above $\tau^{max-comf}$, respectively in (27) and in (28). This discomfort can be monetized using a penalty coefficient ρ (€/°C deviation) as in (30) to be included in the cost minimizing objective function.

$$\min \rho \sum_{t=1}^{T} \tau_t^{dev} \tag{30}$$

In a real implementation setting, some information can be physically obtained and incorporated in the optimization process, e.g., a temperature sensor in the tank.

3.3. Model for air conditioner

A simple yet comprehensive model considering the behavior of the control thermostat of an air conditioner (AC) system is developed according to [25], accounting for the thermostat hysteresis behavior as displayed in Fig. 2 for heating mode, where s_t^{AC} is the *on/off* control variable. The operation depends on the minimum/maximum indoor temperature allowed as well as the building envelope characteristics.

The modeling of an AC requires the following parameters and data:

θ_t^{ext} = outdoor temperature in time t (°C), $t = 0, \cdots, T$.

$\theta^{min}, \theta^{max}$ = *minimum* and *maximum* indoor temperature allowed (°C) (these could be indexed by t according to the user's preferences along the planning period).

P^{AC} = nominal power of the AC appliance (kW).

$\beta = (U.A/C)\Delta t$, where U is the (weighted average) overall heat transfer coefficient of the building unit envelope (kW/(m^2·°C)), A is the surface area of the envelope [m^2], so $U.A$ is the overall thermal conductance of the unit envelope (kW/°C), and C is the overall thermal capacity (kJ/°C).

$\gamma = \chi.\Delta t/C$, where χ is the coefficient of performance of the AC appliance.

The parameters β and γ are computed in the thermal model as in [25].

Decision and auxiliary variables (all for $t = 1, \cdots, T$):

s_t^{AC} = binary *on/off* control variables (s_0^{AC} is a constant).

θ_t^{in} = indoor temperature (°C), (θ_0^{in} is a constant).

y_t, z_t = binary variables to enforce the logical conditions of thermostat switching: $y_t = 1$ if $\theta_t^{in} < \theta^{max}$; $z_t = 1$ if $\theta_t^{in} > \theta^{min}$.

The AC optimization model is:

$$\min \sum_{t=1}^{T} C_t^{buy} P^{AC} s_t^{AC} \Delta t \tag{31}$$

s.t.

$$\theta_t^{in} = (1 - \beta)\theta_{t-1}^{in} + \beta\theta_{t-1}^{ext} + \gamma P^{AC} s_{t-1}^{AC}, \quad t = 1, \cdots, T \tag{32}$$

$$\theta_t^{in} \geq \theta^{min} - \mathscr{M} s_t^{AC}, \quad t = 1, \cdots, T \tag{33}$$

$$\theta_t^{in} \leq \theta^{min} + \mathscr{M} z_t, \quad t = 1, \cdots, T \tag{34}$$

$$\theta_t^{in} \geq \theta^{max} - \mathscr{M} y_t, \quad t = 1, \cdots, T \tag{35}$$

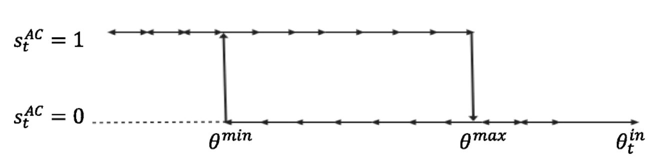

Fig. 2. AC thermostat hysteresis behavior (heating mode).

$$z_t + y_t - s_{t-1}^{AC} + s_t^{AC} \le 2, \quad t = 1, \cdots, T \tag{36}$$

$$z_t + y_t + s_{t-1}^{AC} - s_t^{AC} \le 2, \quad t = 1, \cdots, T \tag{37}$$

$$\theta_t^{in} \le \theta^{max} + \mathscr{M}\left(1 - s_t^{AC}\right), \quad t = 1, \cdots, T \tag{38}$$

$$s_t^{AC}, z_t, y_t \in \{0, 1\}, \quad t = 1, \cdots, T \tag{39}$$

Constraints (32) define the indoor temperature in each time t as a function of the indoor temperature, the external temperature and the AC operation in time $t-1$. Constraints (33) ensure that the AC is *on* when the indoor temperature is below the minimum temperature. Constraints (34)–(37) guarantee that the system keeps the state *on* or *off* when the indoor temperature is between the lower and the upper bound of the thermostat dead-band. Constraints (38) force $s_t^{AC} = 0$ when the indoor temperature is above the maximum allowed temperature, turning the AC *off*.

In this model, the AC is operated in an *on/off* mode. If the AC can operate in, e.g., 4 power levels of 25 or 50 or 75 or 100%, then $P^{AC} s_{t-1}^{AC}$ in (32) is replaced by P_{t-1}^{AC} (with P_0^{AC} being a constant), which is computed as in (40) using the auxiliary variables σ_t^k that establish the power level at which the AC operate. Constraints (42) guarantee that the AC functions at one of the specified power levels or it is *off*.

$$P_t^{AC} = \left(0.25\sigma_t^1 + 0.5\sigma_t^2 + 0.75\sigma_t^3 + \sigma_t^4\right) P^{AC}, \quad t = 1, \cdots, T \tag{40}$$

$$\sigma_t^k \in \{0, 1\}, k = 1, \cdots, 4, \quad t = 1, \cdots, T \tag{41}$$

$$s_t^{AC} = \sum_{k=1}^{4} \sigma_t^k, \quad t = 1, \cdots, T \tag{42}$$

A monetized discomfort term could also be implemented as we illustrated for the EWH. Other models for AC control are presented in [25], for instance, to impose a minimum time *on* or *off*.

However, the model above is just the MILP implementation of a rule-based system to reflect the thermostat behavior using the auxiliary binary variables y_t and z_t, i.e., it does not allow for the exploitation of the consumer's willingness to trade-off some discomfort with lower price periods. For this purpose, the model can be reformulated as follows [24]. The minimum indoor temperature for which the system should turn on (θ^{min} or θ_t^{min}) becomes a decision variable to be determined by the optimization model. The reference (desired target) temperature, θ^{ref}, the maximum allowed for the indoor temperature, θ^{max}, and the absolute minimum allowed indoor temperature, θ^{min_ABS}, are specified by the consumer. The variables δ_t^+ and δ_t^- are the positive and negative deviations of the minimum temperature, θ_t^{min}, to be set by the optimization model, with respect to the reference temperature. These variables account for the discomfort felt by the consumer, which may be included in the consumer's overall cost objective function by monetizing those temperature deviations or considered as a separate objective function in a bi-objective model. Fig. 3 displays this type of control of the lower bound of the thermostat comfort band (AC in heating mode), at each time t of T, by considering θ_t^{min} a decision variable.

The modeling of this additional degree of freedom, in which the optimal value of θ_t^{min} is determined by the model, is achieved by defining

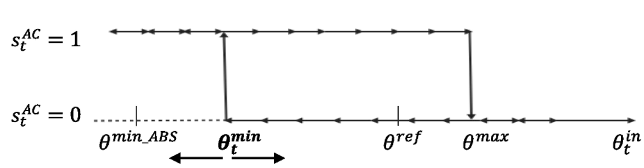

Fig. 3. Control of the lower bound of the thermostat (heating mode) at each time t of T.

the discomfort variables δ_t^+ and δ_t^- as in (43) and guaranteeing that the minimum temperature is within the bounds defined by the absolute minimum temperature and the maximum temperature allowed (44).

$$\theta_t^{min} - \theta^{ref} = \delta_t^+ - \delta_t^-, \quad t = 1, \cdots, T \tag{43}$$

$$\theta^{min\_ABS} \le \theta_t^{min} \le \theta^{max}, \quad t = 1, \cdots, T \tag{44}$$

$$\delta_t^-, \delta_t^+ \ge 0, \quad t = 1, \cdots, T \tag{45}$$

A monetary term penalizing the temperature deviation (46) is added to the cost objective function to be minimized.

$$\min \sum_{t \in \mathrm{T}} \left(c^+ \delta_t^+ + c^- \delta_t^-\right) \tag{46}$$

The coefficients c^+ and c^- are the costs (in €/°C.h) associated with the positive and negative temperature deviations, respectively (e.g., in heating mode it may be set $c^- > c^+$, i.e., negative deviations are more penalized).

The computational complexity results from considering $\theta_t^{min}, t = 1, \cdots, T$, as decision variables, thus allowing to profit from ToU prices while tolerating some discomfort. It may be beneficial to increase θ_t^{min} to heat the space in periods of low prices to have higher temperatures (comfort) in periods of high prices. This end-user flexibility enables the implementation of price-based demand response actions.

3.4. Model for static and electric vehicle battery

Let x denote the type of battery: $x \in \{B, V\}$, where B refers to the static battery and V to the EV battery. Regarding the time domain T_x of each battery, $\mathrm{T}_B = \mathrm{T}$ (the whole planning period) and $\mathrm{T}_V = [t_a, t_d]$ where t_a is the first time unit after *arrival* of the EV at home (enabling charging/discharging) and t_d is the time of *departure*.

In the model below, the battery status is given in energy (kWh) units.

The modeling of the battery systems requires the following parameters and data:

$\eta_x^{ch}, \eta_x^{dch}$ = *charging* and *discharging* efficiency of the battery, $x \in \{B, V\}$.

E_x^{min}, E_x^{max} = *minimum* and *maximum* allowed battery charge (kWh), $x \in \{B, V\}$.

E_x^0 = initial battery charge (kWh) at time $t = 0$ for $x = B$ and $t = t_a - 1$ for $x = V$.

E_x^{req} = battery charge requested at the end of the planning period for $x = B$ and at the time of departure t_d for $x = V$ (kWh); in the case of $x = B$, we consider that $E_B^{req} = E_B^0$.

$P_x^{ch\_max}, P_x^{dch\_max}$ = *maximum charge* and *maximum discharge* power allowed for the battery (kW), $x \in \{B, V\}$.

The decision and auxiliary variables necessary are (for $t \in T_x$, $x \in \{B, V\}$):

P_t^{x2H} = power (kW) such that $P_t^{x2H} \Delta t$ is the energy transferred from the battery x to home (B2H or V2H) in time t (battery discharge).

P_t^{H2x} = power (kW) such that $P_t^{H2x} \Delta t$ is the energy transferred from the home to the battery x (H2B or H2V) in time t (battery charge).

$E_{x,t}$ = energy (kWh) in the battery x in time t ($E_{x,0} = E_x^0$ is a constant as defined above).

s_t^{H2x} = binary variables equal to 1 when the battery x is charging in time t.

s_t^{x2H} = binary variables equal to 1 when the battery x is discharging in time t.

The constraints modeling the operation of the static and the EV batteries are:

$$E_{x,t} = E_{x,t-1} + \left(\eta_x^{ch} P_t^{H2x} \Delta t\right) - \left(\frac{P_t^{x2H} \Delta t}{\eta_x^{dch}}\right), \quad t \in T_x, \quad x \in \{B, V\} \tag{47}$$

$$E_x^{min} \le E_{x,t} \le E_x^{max}, \quad t \in T_x, \quad x \in \{B, V\} \tag{48}$$

$$0 \le P_t^{H2x} \le P_x^{ch\_max} s_t^{H2x}, \quad t \in T_x, \quad x \in \{B, V\} \tag{49}$$

$$0 \le P_t^{x2H} \le P_x^{dch\_max} s_t^{x2H}, \quad t \in T_x, \quad x \in \{B, V\} \tag{50}$$

$$s_t^{H2x} + s_t^{x2H} \le 1, \quad t \in T_x, \quad x \in \{B, V\} \tag{51}$$

$$E_{B,T} \ge E_B^{req}; \; E_{V,t_d} \ge E_V^{req} \tag{52}$$

$$s_t^{H2x}, s_t^{x2H} \in \{0, 1\}, \; t \in T_x, \; x \in \{B, V\} \tag{53}$$

Constraints (47) determine the energy in the batteries considering the charging/discharging process. Constraints (48) impose a minimum and maximum energy quantity in the batteries in each time unit. Constraints (49) and (50) limit the maximum charging ($s_t^{H2x} = 1$) and discharging ($s_t^{x2H} = 1$) rates, respectively. Constraints (51) establish that the batteries are operating in one mode only (charging or discharging) in each time unit. Constraints (52) enforce that the energy in the batteries cannot be lower than the required quantity at the end of the planning period (for the static battery) and at the time of departure (for the EV battery).

4. Overall model and case study

The MILP modules presented in the previous sections can be combined in an overall model to make the integrated optimization of all energy resources (different load types, storage and local micro-generation, exchanges with the grid). These modules can be combined and adapted according to the resources available for control, the consumer's preferences and the aims of the study. In the following version of a comprehensive overall model, we consider also the possibility of selling back to the grid at a stipulated price, which in some countries is a fraction of the wholesale market price. The following additional parameters, data and decision variables (all for $t = 1, \cdots, T$) are required to model all the exchanges.

Additional parameters and data:

B_t = base load (non-controllable) (kW).

P_t^{PV} = power (kW) such $P_t^{PV}\Delta t$ is the local PV energy generation in time t (kWh).

C_t^{sell} = energy remuneration (selling to the grid) in time t (€/kWh).

P^{G_max} = maximum power allowed for exchanges with the grid (kW).

Decision and auxiliary variables:

P_t^{G2H} = power (kW) such that $P_t^{G2H}\Delta t$ is the energy (kWh) transferred from grid to home (G2H) in time t at unit cost C_t^{buy} (€/kWh).

P_t^{H2G} = power (kW) such that $P_t^{H2G}\Delta t$ is the energy (kWh) transferred from home to grid (H2G) in time t at unit cost C_t^{sell} (€/kWh).

s_t^{G2H} = binary variables that are 1 when the energy is flowing from grid to home in time t.

s_t^{H2G} = binary variables that are 1 when the energy is flowing from home to grid in time t.

Also, in addition to the energy cost (€/kWh), the power cost may also be considered by establishing a power tariff structure (€/kW per day) consisting of L price levels and the consumer is charged by the peak power taken. For this purpose, the following additional parameters and decision variables are defined:

C_l^{Cont} = power level prices (€/kW); the consumer is charged for the peak power taken, $l = 1, \cdots, L$.

P_l^{Cont} = power levels (kW), $l = 1, \cdots, L$.

u_l^{Cont} = binary variables defining the maximum power level l taken during the planning period, $l = 1, \cdots, L$.

The constraints to determine the power level to be used are:

$$P_t^{G2H} \le \sum_{l=1}^{L} P_l^{Cont} . u_l^{Cont}, \quad t = 1, \cdots, T \tag{54}$$

$$\sum_{l=1}^{L} u_l^{Cont} = 1 \tag{55}$$

$$u_l^{Cont} \in \{0, 1\}, \quad l = 1, \cdots, L \tag{56}$$

The power cost could also be considered as a constant but imposing an upper bound on the power taken by means of a constraint as established in the contract with the retailer, which is usual in the tariff system of several countries.

The overall model is (57)-(64):

$$\min_{P^{G2H}, P^{H2G}} f = \sum_{t=1}^{T} \left[\left(C_t^{buy} P_t^{G2H} \Delta t \right) - \left(C_t^{sell} P_t^{H2G} \Delta t \right) \right] + \sum_{l=1}^{L} \left(C_l^{Cont} u_l^{Cont} \right) \tag{57}$$

s. t.

$$\begin{array}{l} \text{Constraints of model M3 for shiftable loads: } (9)-(12) \text{ for single (or } (13)-(16) \text{ for multiple) comfort time slots.} \\ \text{Constraints } (19)-(26) \text{ for the EWH load.} \\ \text{Constraints } (32)-(39) \text{ for the AC load.} \\ \text{Constraints } (47)-(53) \text{ for the static battery and the EV battery.} \\ \text{Constraints } (54)-(56) \text{ for the power component.} \end{array} \tag{58}$$

$$0 \le P_t^{G2H} \le P^{G\_max} s_t^{G2H}, t = 1, \cdots, T \tag{59}$$

$$0 \le P_t^{H2G} \le P^{G\_max} s_t^{H2G}, t = 1, \cdots, T \tag{60}$$

$$s_t^{G2H} + s_t^{H2G} \le 1, t = 1, \cdots, T \tag{61}$$

$$P_t^{G2H} - P_t^{H2G} + P_t^{PV} = B_t + \sum_{j=1}^{J} P_{j,t}^{Sh} + P^{AC} s_t^{AC} + P^R v_t + \left(P_t^{H2B} - P_t^{B2H} \right) + \left(P_t^{H2V} - P_t^{V2H} \right), \; \forall t \in T_V \tag{63}$$

$$P_t^{G2H} - P_t^{H2G} + P_t^{PV} = B_t + \sum_{j=1}^{J} P_{j,t}^{Sh} + P^{AC} s_t^{AC} + P^R v_t + \left(P_t^{H2B} - P_t^{B2H}\right), \forall t \in \mathrm{T} \backslash T_V \tag{62}$$

$$s_t^{G2H}, s_t^{H2G} \in \{0, 1\}, t = 1, \cdots, T \tag{64}$$

Constraints (59) – (61) limit the exchanges between the home and the grid to a maximum and impose that the flow occurs in only one direction (i.e., G2H or H2G). Constraints (62) and (63) model the power balance, just differing in the operation slot of the EV battery.

Constraints (27)–(29) could be included in the model to represent the discomfort the consumer would be willing to tolerate with respect to the hot water temperature comfort range, adding the corresponding penalty term (30) to the objective function. Constraints (43)–(45) could be considered to exploit the consumer's willingness to endure some indoor temperature discomfort, which would be penalized in the objective function as in (46), profiting from lower price periods.

This overall model was instantiated with the data available at https://home.deec.uc.pt/~ch/data_DRmodels, obtained in field audits and actual equipment technical specifications. The planning horizon discretization was $\Delta t = 1/60$h, to compute the case study results presented below (which can be entirely reproduced using the data file and the formulation (57)–(64) above). The model has 16,847 binary variables, 21,600 continuous variables and 39,227 constraints. With 5 min runtime, the relative MIP gap was 0.0107, and with 1 hour runtime the gap was 0.0088. The corresponding cost objective function values were 4.0714€ and 4.0697€, respectively.

The evolution of grid to home (P_t^{G2H}) and home to grid (P_t^{H2G}) powers is displayed in Fig. 4. Fig. 5 displays the evolution of the static ($E_{B,t}$) and EV ($E_{V,t}$) battery charge. Fig. 6 displays the indoor temperature (θ_t^{in}) and the EWH temperature (τ_t) in the planning period. These results were obtained with 1 hour runtime, although they are very similar to the ones obtained with 5 min runtime.

Purchase from the grid (P_t^{G2H}) is made in the lower price periods, selling to the grid (P_t^{H2G}) when the prices are higher using the PV generation and the energy stored in the battery. The static battery ($E_{B,t}$) is charged in the lower price periods to supply loads operating in periods in which the energy cost is higher. The EV battery ($E_{V,t}$) is used to supplement the supplying of some loads during high prices periods and is then charged from the grid in low price periods to reach the desired state of charge at the time required. The indoor temperature (θ_t^{in}) fluctuates in the comfort range, being the AC supplied by the grid in periods of low prices and by the battery in periods of high prices. The EWH is mostly supplied from the grid in low price periods considering water withdrawals.

The EWH modeling is responsible for the major share of the computational effort. Without considering the EWH, the overall model would be solved to optimality in 1.36 s.

Further computational experiments were carried out to assess the impact of consumer's comfort specifications on the cost objective function. For this purpose, relaxations of the minimum allowed indoor and hot water temperatures, and minimum battery charge requested at the time of departure of the EV were considered, thus simulating a consumer willing to trade-off comfort for cost. These results are presented in Table 2, for 5-minute runtime, making of most of the model flexibility to assess the outcomes for distinct consumer profiles characterized by different comfort requirements. Accepting to lower the minimum comfort temperature in 1 °C for the indoor and 2 °C for the hot water temperature enables to achieve some gain in cost, with a more noticeable improvement resulting from lowering the requirements for the electric vehicle battery charge at the departure time. The cumulative effect of these three preference settings offer a significant saving of about 12.6% with respect to the original settings (please see the data file).

Experiments were also made using a plain tariff with $\overline{C}^{buy} = \frac{1}{T}\sum_{t=1}^{T} C_t^{buy}$. Allowing for a running time of 5 min, the cost objective function was 7.1284€, which shows that ToU tariff schemes are favorable for consumers when they have the flexibility or the willingness to endure some discomfort associated with appliance operation shifting, indoor and hot water temperatures, or battery state of charge requirements.

5. Conclusions

The integrated optimization of all energy resources (load management, electric vehicle and stationary battery, local microgeneration, exchanges with the grid) to be implemented in autonomous home energy management systems requires an accurate modeling of appliances' physical operation. However, a balance is necessary between the

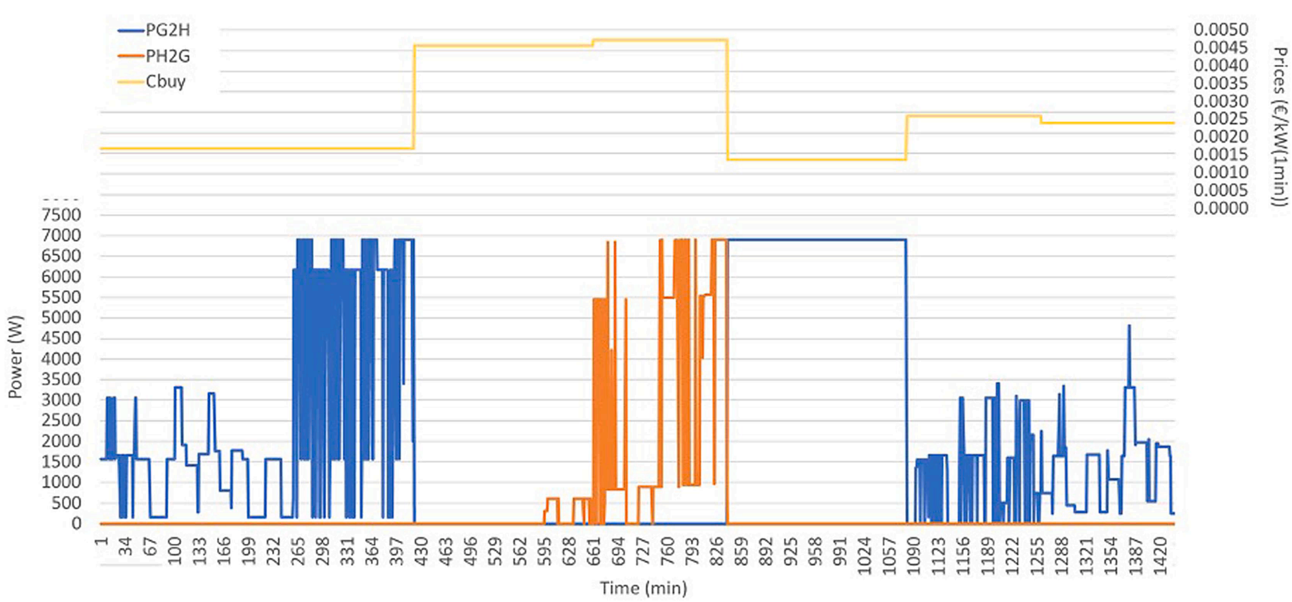

Fig. 4. Grid to home power (P_t^{G2H}) and home to grid (P_t^{H2G}) power.

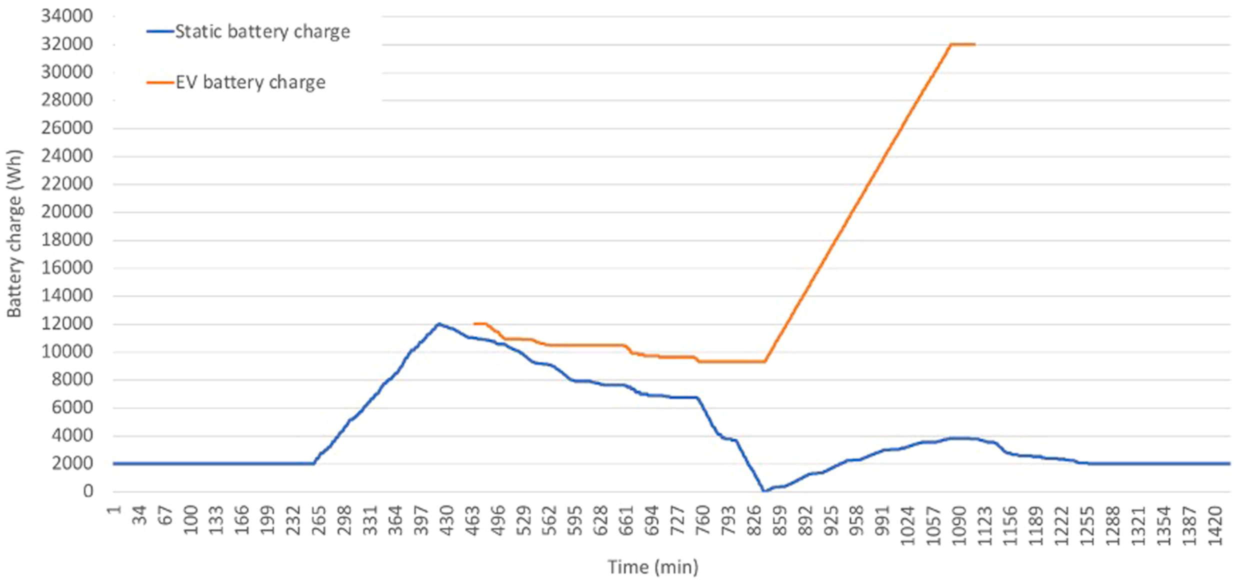

Fig. 5. Evolution of static ($E_{B,t}$) and EV ($E_{V,t}$) battery charge.

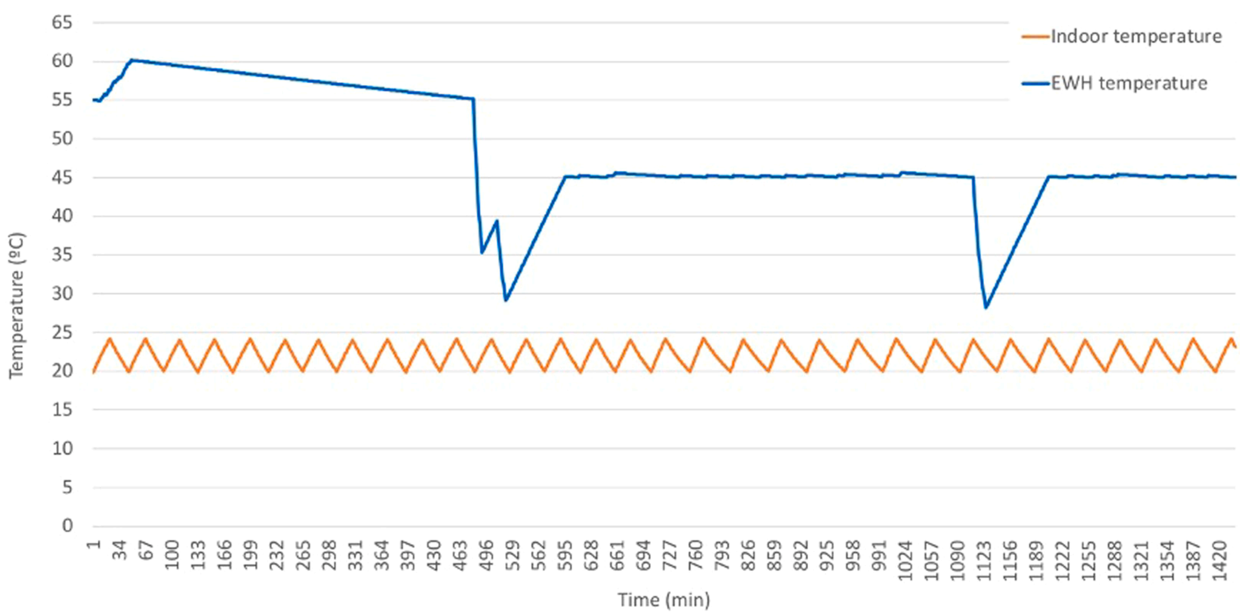

Fig. 6. Evolution of the indoor temperature (θ_t^{in}) and the EWH temperature (τ_t).

Table 2
Results for the overall model with different comfort parameterizations (5-minute runtime).

	MIP gap	Cost	Cost improvement
Original model	0.0107	4.0714	—
$\theta^{min} = 19$ °C instead of 20 °C	0.0105	3.9451	3.1%
$\tau^{min} = 43$ °C instead of 45 °C	0.0104	3.9945	1.9%
$E_V^{req} = 30$ kWh instead of 32 kWh	0.0114	3.7571	7.7%
$\theta^{min} = 19$ °C and $\tau^{min} = 43$ °C	0.0106	3.8699	4.9%
$\theta^{min} = 19$ °C, $\tau^{min} = 43$ °C and $E_V^{req} = 30$ kWh	0.0114	3.5572	12.6%

optimization model detail and the capability of obtaining practical solutions using mild computational requisites. For this purpose, a comprehensive and modular set of MILP models has been developed. The models have been designed to be used in a flexible building block manner, with objective functions involving the economic and comfort dimensions with different modeling approaches. These models can be easily adapted to specific circumstances, including appliance characteristics, comfort preferences (in the operation time, indoor and water temperature, and battery state of charge), time-differentiated tariff schemes, power cost structures, etc. Results of a case study with actual data are presented, with complete data sets provided. The results show that whenever consumers have the flexibility to change their consumption patterns, they are able to lower the net electricity bill by having an energy management system endowed with the models herein proposed to make optimized decisions on their behalf.

Since combinatorial models impose a significant computational effort, a tradeoff is required between the computational resources available and the model accuracy, namely regarding the time interval discretization. The implementation of these models in a low-cost single board computer, such as Arduino or Raspberry Pi, is underway, including the communication with the appliances, thus offering practical and affordable solutions for consumers and prosumers to engage in demand response programs and play a more active role in the energy transition.

CRediT authorship contribution statement

Carlos Henggeler Antunes: Writing – original draft, Investigation, Conceptualization, Data curation. **Maria João Alves:** Writing – review & editing, Investigation, Conceptualization. **Inês Soares:** Writing – review & editing, Investigation, Software.

Declaration of Competing Interest

The authors declare that they have no known competing financial interests or personal relationships that could have appeared to influence the work reported in this paper.

Acknowledgments

This work was supported by the R&D Units Pluriannual Funding UIDB/00308/2020 and UIDB/05037/2020, and project grants MAnAGER (POCI-01- 0145-FEDER-028040) and RETROSIM (POCI-01-0145-FEDER-032503), through the European Social Fund, European Regional Development Fund and the COMPETE 2020 Programs, FCT- Portuguese Foundation for Science and Technology.

References

[1] Siano P. Demand response and smart grids—A survey. Renew Sustain Energy Rev 2014;30:461–78. https://doi.org/10.1016/j.rser.2013.10.022.
[2] Vardakas JS, Zorba N, Verikoukis CV. A Survey on Demand Response Programs in Smart Grids: Pricing Methods and Optimization Algorithms. IEEE Commun Surv Tutorials 2015;17(1):152–78. https://doi.org/10.1109/COMST.2014.2341586.
[3] Jordehi AR. Optimisation of demand response in electric power systems, a review. Renew Sustain Energy Rev 2019;103:308–19. https://doi.org/10.1016/j.rser.2018.12.054.
[4] Beaudin M, Zareipour H. Home energy management systems: A review of modelling and complexity. Renew Sustain Energy Rev 2015;45:318–35. https://doi.org/10.1016/j.rser.2015.01.046.
[5] Hussain M, Gao Y. A review of demand response in an efficient smart grid environment. Electr J 2018;31(5):55–63. https://doi.org/10.1016/j.tej.2018.06.003.
[6] Morales-España G, Martínez-Gordón R, Sijm J. Classifying and modelling demand response in power systems. Energy 2022;242:122544. https://doi.org/10.1016/j.energy.2021.122544.
[7] Althaher S, Mancarella P, Mutale J. Automated Demand Response From Home Energy Management System Under Dynamic Pricing and Power and Comfort Constraints. IEEE Trans Smart Grid 2015;6(4):1874–83. https://doi.org/10.1109/TSG.2014.2388357.
[8] Merdanoğlu H, Yakıcı E, Doğan OT, Duran S, Karatas M. Finding optimal schedules in a home energy management system. Electr Power Syst Res 2020;182:106229. https://doi.org/10.1016/j.epsr.2020.106229.
[9] Salgado M, Negrete-Pincetic M, Lorca Á, Olivares D. A low-complexity decision model for home energy management systems. Appl Energy 2021;294:116985. https://doi.org/10.1016/j.apenergy.2021.116985.
[10] Nan S, Zhou M, Li G. Optimal residential community demand response scheduling in smart grid. Appl Energy 2018;210:1280–9. https://doi.org/10.1016/j.apenergy.2017.06.066.
[11] Adhikari R, Pipattanasomporn M, Rahman S. An algorithm for optimal management of aggregated HVAC power demand using smart thermostats. Appl Energy 2018;217:166–77. https://doi.org/10.1016/j.apenergy.2018.02.085.
[12] Shafie-Khah M, Siano P. A Stochastic Home Energy Management System Considering Satisfaction Cost and Response Fatigue. IEEE Trans Ind Informatics 2018;14(2):629–38. https://doi.org/10.1109/TII.2017.2728803.
[13] Elkazaz M, Sumner M, Naghiyev E, Pholboon S, Davies R, Thomas D. A hierarchical two-stage energy management for a home microgrid using model predictive and real-time controllers. Appl Energy 2020;269:115118. https://doi.org/10.1016/j.apenergy.2020.115118.
[14] Javadi MS, Nezhad AE, Nardelli PHJ, Gough M, Lotfi M, Santos S, et al. Self-scheduling model for home energy management systems considering the end-users discomfort index within price-based demand response programs. Sustain Cities Soc 2021;68:102792. https://doi.org/10.1016/j.scs.2021.102792.
[15] Zhang X, Lu R, Jiang J, Hong SH, Song WS. Testbed implementation of reinforcement learning-based demand response energy management system. Appl Energy 2021;297:117131. https://doi.org/10.1016/j.apenergy.2021.117131.
[16] Mohseni A, Mortazavi SS, Ghasemi A, Nahavandi A, Talaei abdi M. The application of household appliances' flexibility by set of sequential uninterruptible energy phases model in the day-ahead planning of a residential microgrid. Energy 2017;139:315–28. https://doi.org/10.1016/j.energy.2017.07.149.
[17] Soares A, Gomes A, Antunes CH, Oliveira C. A Customized Evolutionary Algorithm for Multi-Objective Management of Residential Energy Resources. IEEE Trans Ind Informatics 2017;13(2):492–501. https://doi.org/10.1109/TII.2016.2628961.
[18] Deng R, Yang Z, Chow M-Y, Chen J. A Survey on Demand Response in Smart Grids: Mathematical Models and Approaches. IEEE Trans Ind Informatics 2015;11(3):570–82. https://doi.org/10.1109/TII.2015.2414719.
[19] Niromandfam A, Yazdankhah AS, Kazemzadeh R. Modeling demand response based on utility function considering wind profit maximization in the day-ahead market. J Clean Prod 2020;251:119317. https://doi.org/10.1016/j.jclepro.2019.119317.
[20] Feng C, Wang Y, Zheng K, Chen Q. Smart Meter Data-Driven Customizing Price Design for Retailers. IEEE Trans Smart Grid 2020;11(3):2043–54. https://doi.org/10.1109/TSG.2019.2946341.
[21] Soares A, Gomes Á, Antunes CH. Categorization of residential electricity consumption as a basis for the assessment of the impacts of demand response actions. Renew Sustain Energy Rev 2014;30:490–503. https://doi.org/10.1016/j.rser.2013.10.019.
[22] Henggeler Antunes C, Alves MJ, Ecer B. Bilevel optimization to deal with demand response in power grids: models, methods and challenges. TOP 2020;28(3):814–42. https://doi.org/10.1007/s11750-020-00573-y.
[23] Alves MJ, Antunes CH, Carrasqueira P. A hybrid genetic algorithm for the interaction of electricity retailers with demand response. In: in *Applications of Evolutionary Computation, 19th European Conference (EvoApplications), Lecture Notes in Computer Science 9597*; 2016. p. 459–74.
[24] Soares I, Alves MJ, Antunes CH. Designing time-of-use tariffs in electricity retail markets using a bi-level model – Estimating bounds when the lower level problem cannot be exactly solved. Omega 2020;93:102027. https://doi.org/10.1016/J.OMEGA.2019.01.005.
[25] Antunes CH, Rasouli V, Alves MJ, Gomes Á, Costa JJ, Gaspar A. A Discussion of Mixed Integer Linear Programming Models of Thermostatic Loads in Demand Response. In: Bertsch V, editor. Advances in Energy System Optimization, Trends in Mathematics. Cham: Birkhäuser (Springer); 2020. p. 105–21.
[26] Tejero-Gómez JA, Bayod-Rújula AA. Energy management system design oriented for energy cost optimization in electric water heaters. Energy Build 2021;243:111012. https://doi.org/10.1016/j.enbuild.2021.111012.